applied sciences

MDPI

Article

Analysis of Acoustic Emission Waveforms by Wavelet Packet Transform for the Detection of Crack Initiation Due to Fretting Fatigue in Solid Railway Axles

Marta Zamorano [1,*], María Jesús Gómez [2], Cristina Castejon [2] and Michele Carboni [3]

[1] Higher Polytechnic School, Universidad Francisco de Vitoria, Crta. Pozuelo-Majadahonda km 1,800, 28223 Pozuelo de Alarcón, Madrid, Spain
[2] Mechanical Engineering Department, Universidad Carlos III de Madrid, Avda. Universidad 30, 28911 Leganés, Madrid, Spain; mjggarci@ing.uc3m.es (M.J.G.); castejon@ing.uc3m.es (C.C.)
[3] Department Mechanical Engineering, Politecnico di Milano, Via La Masa 1, 20156 Milano, Italy; michele.carboni@polimi.it
* Correspondence: marta.zamorano@ufv.es

Abstract

Railway axles are among the most safety-critical components in rolling stock, as their failure can lead to catastrophic consequences. One of the most subtle damage mechanisms affecting these components is fretting fatigue, which is a particularly challenging damage mechanism in these components, as it can initiate cracks under real service conditions and is difficult to detect in its early stages, which is vital to ensure operational safety and to optimize maintenance strategies. This paper focuses on the development of fretting fatigue damage in solid railway axles under realistic service-like conditions. Full-scale axle specimens with artificially induced notches were subjected to loading conditions that promote fretting fatigue crack initiation and growth. Acoustic emission techniques were used to monitor the damage progression, and post-processing of the emitted signals, by using wavelet-based tools, was conducted to identify early indicators of crack formation. The experimental findings demonstrate that the proposed approach allows for reliable identification of fretting-induced crack initiation, contributing valuable insights into the in-service behavior of railway axles under this damage mechanism.

Keywords: fretting fatigue; solid railway axle; acoustic emission; wavelet packet transform; ensemble bagged trees

Academic Editor: Andrea Carpinteri

Received: 18 June 2025
Revised: 21 July 2025
Accepted: 29 July 2025
Published: 29 July 2025

Citation: Zamorano, M.; Gómez, M.J.; Castejon, C.; Carboni, M. Analysis of Acoustic Emission Waveforms by Wavelet Packet Transform for the Detection of Crack Initiation Due to Fretting Fatigue in Solid Railway Axles. *Appl. Sci.* **2025**, *15*, 8435. https://doi.org/10.3390/app15158435

1. Introduction

Ensuring proper maintenance of a railway axle is crucial, as it is a key safety component. Detecting fatigue cracks, able to quickly propagate to failure in axles during service, is currently one of the most significant research areas in the railway field. Nevertheless, according to relevant standards [1,2], axle design still follows the traditional fatigue limit concept with the consequence that initiation and propagation of cracks, along with failures, are still observed from time to time.

This work addresses the phenomenon of fretting fatigue damage [3–6] in railway axles, which refers to the repeated micro-sliding between two contacting surfaces in a press-fit connection, caused by applied loads and vibrations. Damage, then, starts with the onset of wear and gradually progresses to the formation of microcracks. These can develop into larger surface cracks that may propagate, depending on the applied load, leading to a

significant reduction in fatigue life [3,7,8]. In railway wheelsets, this phenomenon can lead to unexpected early failures, typically occurring at the interfaces between the axle and the press-fitted wheels, brakes, or gear wheels [9,10]. For this reason, various approaches have been proposed over time to address fretting fatigue in railway axles [11], including design modifications and maintenance operations based on non-destructive testing (NDT) techniques during service interruptions [12]. However, the current trend favors condition-based monitoring, as it enables real-time or on-demand structural health monitoring (SHM) tools and methods to be applied without interrupting service or disassembling the axles, resulting in cost savings.

At present, only a limited number of studies focuses on SHM applied to railway axles. These studies, in terms of methodological approach, primarily utilize acoustic emission (AE) [13–17], low frequency vibrations [18], high frequency vibrations [19] and automated ultrasonic testing (UT) [20,21]. The only found research specifically addressing fretting fatigue damage monitored through AE is research work by the current authors [22]. The advantages of AE [23] lie in its proven effectiveness across various technical fields and its use of compact, easy-to-handle equipment. However, its main drawback is the vast amount of data generated, which must be managed and interpreted, as not all recorded signals are related to damage developing in the material. Therefore, clustering and classification techniques are typically required to interpret and extract useful data [22,24]. From the point of view of signal processing for the case at hand, numerous studies have explored and applied wavelet techniques to detect damage in various applications [25–27], some of which are specifically tailored for analyzing AE signals [28–31]. These approaches are particularly effective for analyzing AE signals associated with the damage initiation phase (static or cyclic plasticity leading to initial material cracking) and the final failure phase (rapid and unstable crack propagation). Both stages are typically marked by high-energy AE events, whereas the stable propagation phase is known to be much more silent [32,33]. A beneficial outcome is that, during the initiation and final failure stages, AE signals related to noise or other non-failure phenomena generally have minimal impact on the overall energy trend of AE events [34]. This is why the acquired waveforms can often be analyzed directly without the need to first classify or cluster out unwanted signals.

The Wavelet Packet Transform (WPT) is one of the most widely used tools in defect detection, often relying on the energy content of signals. Additionally, a key advantage of wavelet-based techniques is their ability to function as a filtering process, enhancing the signal-to-noise ratio and enabling the extraction of features from complex signals. The WPT offers the advantage of allowing the wavelet transform to be applied multiple times by selecting the decomposition level, resulting in enhanced filtering. This is why it has been utilized in several studies [35–37]. One of the primary challenges with these techniques is determining the optimal parameters, such as the mother wavelet and decomposition level, for effective analysis. Early studies on wavelets and AE revealed [26] that better results were achieved when the mother wavelet closely resembled the original AE waveform. The Symlet wavelet of order 8 was found to be suitable when a single pulse generated the wave, whereas the Daubechies db40 wavelet was more appropriate for waves generated by bursts [38]. Consequently, several studies on AE signals have examined the selection of the optimal mother wavelet [39], but, as there is no universally optimal mother wavelet for AE signals yet, it is essential to develop a methodology that selects the best one for each specific case. This will be the focus of this work, as ease and speed of detection are crucial for enhancing the monitoring process. When it comes to decomposition levels, higher levels require more computation time, which may not be suitable for continuous monitoring tasks. Therefore, selecting the optimal parameters for the wavelet technique is vital to ensure a faster and more efficient diagnosis during service.

The present study addresses AE applied to monitor fretting fatigue damage in solid railway axles, a topic for which no related works have been identified in the literature, apart, as said, from a previous study proposed by the current authors [22]. Such a study centered on the application of an unsupervised classification algorithm to AE acquisitions gathered during a full-scale fatigue test performed using a three-point rotating bending bench (Vitry test rig). Artificial notches were introduced into the tested axle to initiate and propagate fretting fatigue damage until significant fatigue cracks developed. The algorithm applied initial clustering, based on a pattern recognition approach, to isolate signals related to potential damage, which proved to be challenging. While the approach was ultimately successful, it required post-processing of experimental data, making it less suitable for early in-service damage detection and resulting in a slower overall procedure. In contrast, the current work proposes a new, structured signal analysis workflow aimed at achieving fast and reliable crack initiation detection for in-service monitoring. This methodology includes: (1) selecting optimal WPT parameters using a supervised classification model based on ensemble bagged trees; (2) assigning class labels according to temporal segmentation of AE data, supported by change point analysis (CPA) on signal energy to differentiate early and advanced fatigue stages; (3) applying the selected WPT parameters for feature extraction from raw AE signals; and (4) employing the trained classifier to detect crack initiation in real time without the need for prior noise filtering or clustering. This approach enhances automation and efficiency in condition-based monitoring of railway axles.

2. Description of the Experimental Full-Scale Test

This section summarizes the experimental full-scale test conducted to monitor the fretting fatigue phenomenon in axles, along with a description of the used AE acquisition equipment. As stated above, this test and its results are the same already used for developing and proposing the different post-processing approach described in the previous work by the authors [22] on the topic of interest and, moreover, they were originally part of a broader research program whose full details are available in [40–42]. A summary of the main points, relevant to the present research, is reported in the following.

A full-scale specimen (Figure 1) made from EA4T steel grade (quenched and tempered 25CrMo4 steel) was tested according to the suggestions of standard EN 13261 [43] for press-fitted assemblies to characterize fretting fatigue damage. To simulate typical fretting damage found in real railway axles, four artificial notches, each 350 µm deep, were machined using Electrical Discharge Machining (EDM) 9 mm from the edge of the press-fit seat. These notches were spaced 75° apart circumferentially to assess the propagation behavior of pre-existing defects under the press-fit [44].

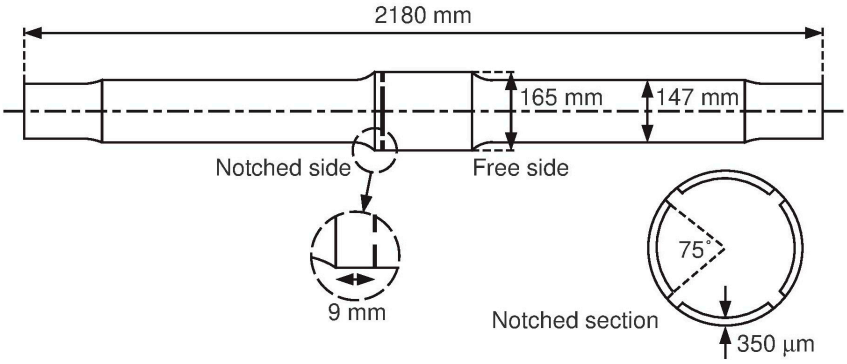

Figure 1. Full scale specimen and artificial notches.

The test was performed using the "Dynamic Test Bench for Railway Axles" (BDA) available at the Department of Mechanical Engineering, Politecnico di Milano. This bench,

a Vitry test rig, applies a three-point rotating bending condition to the specimen. The test operated at a rotational speed of 509 rpm, typical for freight applications. Due to the bench's geometry and configuration, the specimen could not accommodate a real press-fitted full-scale wheel, so a specially designed wheel hub (bush) was used to simulate it.

The test was conducted over a total of 22×10^6 fatigue cycles. A stress of 108 MPa was applied for the first 15×10^6 cycles, after which the stress was increased to 135 MPa until the test's completion to induce the final fracture. This approach was used to ensure the initiation and propagation of fretting fatigue damage [45].

The adopted AE acquisition system (Vallen Systeme AE control unit AMSY-6 with eight channels) continuously monitored the specimen using a single AE sensor (Vallen Systeme VS150-M, Vallen Systeme GmbH, Offenbach am Main, Germany) with a resonance frequency range of 100–450 kHz. Due to spatial constraints, just one sensor was positioned at one of the two free ends of the full-scale specimen using a custom-made mount, which also held a pre-amplifier (Vallen Systeme AEP4, Vallen Systeme GmbH, Offenbach am Main, Germany, 34 dB). The sensor coupling was periodically verified with a Pencil Lead Break (PLB) test [46]. The signals generated by the PLB test displayed a distinct burst waveform with a maximum amplitude of 70 dB.

The acquired signals were transmitted from the rotating parts to the AE acquisition system by a sliding contact (Michigan Scientific S4, Michigan Scientific Corporation, Grand Rapids, MI, USA) and the number of applied fatigue cycles was also recorded. To verify that the contact did not adversely affect the signal quality, the aforementioned periodic Pencil Lead Break (PLB) tests were conducted before and after signal transmission through the slip ring. These tests showed consistent waveform characteristics and energy levels, confirming that the sliding contact did not introduce noticeable signal distortion or attenuation. AE monitoring during the test was managed using Vallen Systeme AE-Suite Software R2017.0504.1.

The proper functioning of the acquisition chain was checked using, again, the PLB test, and the finally adopted acquisition parameters are detailed in Table 1. The acquisition threshold was set to 69 dB to capture signals similar to PLB bursts, while minimizing the collection of unnecessary background noise.

Table 1. AE acquisition parameters.

Parameter	Value
Channel	1
Sampling rate for the acquisition of AE features	10 MHz
Sampling rate for the acquisition of AE transient waveforms	5 MHz
Max samples per set	524,288
Pre-Trigger	200 µs
Acquisition threshold (with respect to a reference voltage amplitude of 1 µV)	69 dB
Frequency filter	230–850 kHz
Pre-Amp gain	34 dB
Rearm Time	3.2 µs

During the test, both wave features and waveforms were recorded for all the acquired raw signals, i.e., those characterized by an amplitude higher than the applied acquisition threshold.

At the conclusion of the test, visual and magnetic particle inspections were performed to assess the condition of the axle. The results, discussed in earlier work [22], are useful for developing and interpreting the findings of the present study. Specifically, two fatigue cracks were detected: a smaller one located on the free side of the full-scale specimen

(Figure 1), being 3 mm from the edge of the press-fit seat and with a 4 mm circumferential extension, and a larger circumferential one originating from both ends of one of the artificial notches. Figure 2 displays the collected AE raw data, alongside the trend of the applied stress during the test.

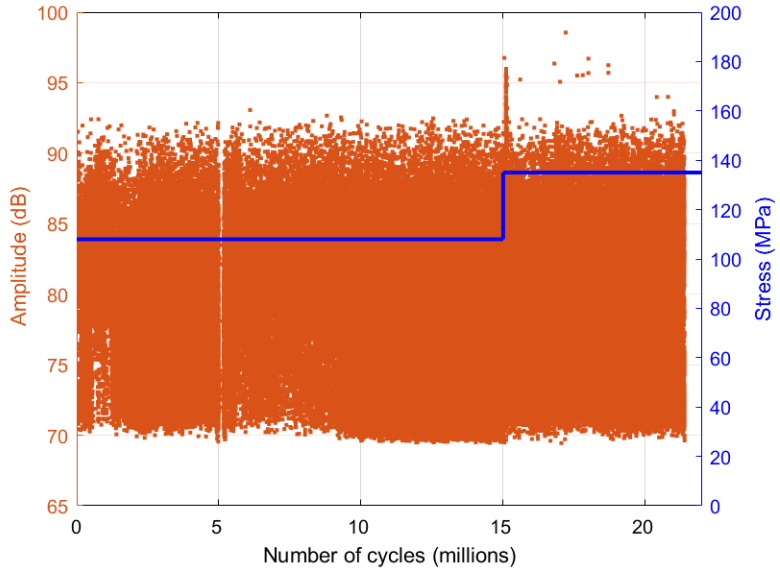

Figure 2. Acoustic emission raw data collected during the test and time history of the applied loading conditions.

3. Wavelet Packet Transform

The Wavelet Transform (WT) is a mathematic tool that presents information in both time and frequency domains, unlike other traditional tools such as Fourier Transform, which only provides insights in the frequency domain [47]. The WT breaks down the signal into various frequency components by applying a translation (τ) and expansion (s) process to a function known as the mother wavelet $\psi(t)$, resulting in the wavelets $\psi_{s,\tau}(t)$ as illustrated in Equation (1) [48]:

$$\Psi s, \tau(t) = \frac{1}{\sqrt{s}} \Psi \left(\frac{1-\tau}{s} \right) \quad (1)$$

Since the signals in this study are measured discretely, it is necessary to apply the Discrete Wavelet Transform (DWT). Using digital filters, which are associated with the mother wavelet, this method decomposes and divides the signal frequency resolution into two equal parts at each level of decomposition. One part corresponds to the approximation (low frequency), while the other represents the detail (high frequency). The technique applied in this work, the Wavelet Packet Transform (WPT) is essentially the DWT applied recursively up to a specified decomposition level k, which determines the number of packets or frequency ranges into which the analyzed frequency is divided $\left(2^k\right)$ (Figure 3), where $W(k, j)$ represents the signal coefficients for each packet, with j indicating the packet's position within the decomposition level (Equation (2)). In this way, the WPT allows performing a filtering process more times on a given signal. This decomposition is achieved by passing the study signal $x[k]$ through a low-pass filter g to obtain the approximation coefficients A with Equation (3), and a high pass filter h to obtain the detail coefficients D with Equation (4) [49], where n is each point of the signal after filtering. In these equations, i represents the coefficient index and N is the total number of coefficients.

$$\mathrm{W(k,j)} = \{w_1(\mathrm{k,j}), \ldots, w_N(\mathrm{k,j})\} = \{w_i(\mathrm{k,j})\} \quad (2)$$

$$A[n] = \sum_{k=-\infty}^{\infty} x[k]g[2n-k] \quad (3)$$

$$D[n] = \sum_{k=-\infty}^{\infty} x[k]h[2n-k] \quad (4)$$

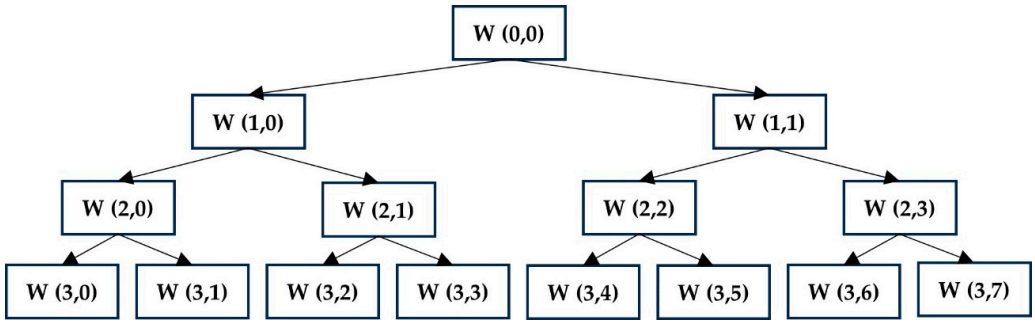

Figure 3. WPT decomposition process for a decomposition level of 3.

Therefore, two key parameters must be selected in advance when using this tool: the mother wavelet and the decomposition level k, both of which significantly influence the results. The importance of such a good selection is demonstrated in some other works [25,50]. To analyze changes in signals corresponding to defects, it is beneficial to work in terms of energy, as this approach provides clearer and more interpretable information. The use of wavelet tools yields a large number of coefficients, making energy analysis particularly useful. Moreover, the energy of the packets has been proved to be an effective feature for detecting changes in the dynamical behavior of the system [50–52]. The energy $E\ (k, j)$, for each packet j at decomposition level k, is computed as the sum of the squares of its coefficients, as described in Equation (5), with additional details provided in Equation (2):

$$\mathrm{E}\ (k, j) = \sum_{\mathrm{i}} [w_i(k, j)]^2 \quad (5)$$

Various families of mother wavelets are discussed in the literature, including classical functions such as Daubechies, Coiflet, Meyer, and others [49]. Each family has distinct characteristics that make it more suitable for certain applications; however, there is no consensus in the literature regarding the optimal choice of mother wavelet for a specific case. For discrete signals and tools, families Daubechies, Symlets, and Coiflets can be used and are the most common [25], and that is why these families will be examined in this work. This analysis will help identify the most appropriate mother wavelet for each case, enabling clearer differentiation between conditions by analyzing the energy of experimental AE signals and optimizing the success rate of an intelligent classification system.

4. Selection of the Mother Wavelet

To conduct an effective WPT analysis, it is essential to select the optimal mother wavelet. For this purpose, a procedure based on the approach presented in a previous study [25] is applied. Although that study focused on vibratory signals, it explored the Daubechies, Symlets, and Coiflets wavelet families, which are particularly well suited for discrete signal processing applications. These wavelet families share several important characteristics that justify their selection in this work.

Firstly, all three families consist of compactly supported wavelets with orthogonal or nearly orthogonal properties, making them ideal for energy-preserving decomposition, which is essential when analyzing energy distribution in AE signals. Additionally, they

offer good time-frequency localization, allowing for the accurate identification of transient events such as burst-type acoustic emissions.

The Daubechies wavelets are known for their ability to represent signals with sharp discontinuities or rapid changes, thanks to their high number of vanishing moments. The Symlets are a modified version of Daubechies wavelets with improved symmetry, which can reduce phase distortion, which is useful for analyzing signals where temporal alignment is important. The Coiflets provide an even higher number of vanishing moments for both the wavelet and scaling functions, enhancing their performance in capturing both smooth and detailed signal components.

These characteristics are particularly relevant for acoustic emission signals, which often exhibit short-duration, high-frequency burst events that resemble wavelet shapes in time [38]. Therefore, the selected families offer the mathematical and practical advantages required for accurate and efficient signal decomposition in the context of damage detection via AE monitoring.

Other wavelet families, such as Biorthogonal, Meyer, or Morlet, were not included in this analysis, as they are either not compactly supported, not orthogonal, or primarily designed for continuous wavelet analysis, making them less suitable for the discrete, energy-based WPT approach used in this work.

For this reason, the same wavelet families will be used in this study. By selecting the appropriate mother wavelet, it will also be able to filter out noise from the signal, eliminating the need for clustering the signals. This approach is particularly advantageous because the damage waveforms are better suited to wavelet transformation. As a result, the detection process can be performed more quickly, a point demonstrated in previous works, which highlighted the similarity between the shape of the wavelet and the burst event generated by defects in the signal.

These studies also focused on a maximum of ten vanishing moments. A comprehensive summary of this parameter can be found in a previous work [25], but in essence, it refers to the fact that within the mother wavelet families, there are wavelets of varying orders, each with distinct properties. For example, the Coiflets family ranges from Coif1 to Coif5, while the Daubechies family spans from db1 to db45. The aforementioned preselection is intended to study all wavelets under the same conditions, as prior research has shown that increasing the number of vanishing moments leads to longer computation times with minimal variation in results. As the aim of this application is condition monitoring of the system, this consideration is important for ensuring a fast and efficient procedure. For the same reason, the decomposition level will be set at 3. In this study, the decomposition level for the WPT was fixed at level 3. This choice is based on a trade-off between time–frequency resolution and computational cost, and is consistent with previous studies [25], that showed level 3 to be effective in capturing the frequency content relevant to different signals while maintaining manageable feature dimensionality.

In WPT, increasing the decomposition level leads to finer frequency resolution, but also to a rapid increase in the number of data (e.g., 2^n data for level n), which can result in redundant information, overfitting, or unnecessary computational load. At level 3, the signal is decomposed into 8 frequency bands, which is typically sufficient to isolate transient high-frequency components associated with crack initiation events in AE signals.

Preliminary comparisons with levels 2 and 4 showed that level 2 lacked sufficient frequency resolution to distinguish subtle differences in AE energy distributions, while level 4 increased feature dimensionality without significantly improving discrimination performance. Therefore, level 3 was selected as a practical and effective compromise for this application.

It is worth noting that, for Symlets and Daubechies families, the order of the mother wavelet coincides with the number of vanishing moments, while, in the Coiflets family, the number of vanishing moments is double the order, which means that Coif4, for example, has 8 vanishing moments, whereas Daubechies 8 has 8 vanishing moments.

For the mother wavelet selection, the following steps have been carried out:

1. First, two different conditions of the axle must be selected (Figure 4). The first class or condition, from now on called "class 0", should be considered at the very beginning of the test, since it is known that the axle has the healthiest condition and there should be no crack initiation yet. The second one, from now on called "class 1", can be considered before the load increase so that it can be analyzed under the same test conditions and that sufficient time has passed for susceptible changes to occur. This selection will be justified with a subsequent change point analysis (CPA) in point 3. During the fretting fatigue test, a continuous acoustic emission (AE) monitoring system recorded a large number of raw signals throughout the cycling process. However, many of these signals corresponded to background noise, frictional contact, or spurious sources unrelated to material degradation. To ensure the relevance and quality of the data analyzed, a manual preselection process was applied and only some of the signals displaying a clear burst-type waveform, characteristic of AE events linked to crack initiation or structural activity, were retained. As a result, a curated dataset of 822 waveforms was obtained: 528 from the healthy condition (class 0), collected during the first 100,000 cycles, and 294 from the early damage condition (class 1), acquired over the subsequent 10,000 cycles. The larger number of waveforms in the healthy class reflects the need for a more comprehensive baseline characterization of the undamaged system, which is essential for assessing deviations associated with incipient damage. Figure 4 shows both selected classes, the number of cycles of each class and the stress conditions applied during the test.
2. WPT with a decomposition level of 3 is applied, with different mother wavelets and the mean energy of the eight obtained packets are calculated, which means that the frequency range is divided into eight equal parts. Considering the sampling frequency shown in Table 1, each packet has a resolution of 3.125×10^5 Hz (2.5×10^6 Hz/8).
3. A change point analysis (CPA) is performed [53] to check the previous selection of classes 0 and 1. This algorithm allows to find noticeable trend changes in the data, according to statistical parameters such as the mean, as in this case (packets energy). It also sets when that change happens. If the energy of all packets is represented for all the selected signals (Figure 5), where the energy of packet 1 (blue) and packet 2 (orange) stand out from the rest and, therefore, contain most of the energy, it can be seen that the selection of the data is well carried out, because there is an increase in the mean energy with class 1. In this way, it is proved that there is a considerable increase in the mean energy from measure 525, which almost corresponds with the beginning of class 1.
4. The DEV value for each mother wavelet is calculated (this parameter was defined in previous work [25]). It measures the difference in energy between two signal conditions: in this case, the healthy condition (i.e., class 0) and another condition taken at a higher number of cycles (i.e., class 1). A higher DEV value indicates a greater energy contrast between both states, meaning the wavelet is more effective at highlighting differences associated with the progression of damage. This is particularly relevant in the context of crack detection, since the key to early and reliable identification of structural changes lies in the ability to discriminate subtle variations in signal features. A wavelet that maximizes the DEV value ensures greater sensitivity to damage, improving the model's ability to differentiate between normal and anomalous

conditions. Therefore, selecting the mother wavelet with the highest DEV is essential for optimizing the performance of the monitoring system (Equation (6)).

$$DEV = \sqrt{\frac{\sum_{i=1}^{n}\left(P_i - O_i\right)^2}{n}} \quad (6)$$

where n is the number of packets, i is the packet number, P_i is the mean energy of packet i for the instantaneous condition (defective), and O_i is the mean energy of packet i for the reference condition (healthy).

5. According to point 4, the mother wavelets (MW) with the highest DEV values will be preselected ($DEVmax$). These values will be used for each MW $DEV(n)$ to calculate the variation in the DEV (DEV(%)) with Equation (7). Those MW with less than 2% variation in the DEV value with respect to the one with the highest DEV value will also be preselected. The choice of the 2% threshold is based on its successful application in previous studies [25], where it provided an effective compromise between sensitivity and selectivity in the context of wavelet-based signal characterization. In this work, the same criterion was adopted to retain mother wavelets whose DEV values were within 2% of the maximum observed value. This threshold ensures that only wavelets with comparable discriminatory power are selected, while preventing the inclusion of marginally relevant ones. Although heuristic in nature, the 2% value was also verified in the present study through preliminary sensitivity analysis, showing that variations in the threshold (e.g., 1% or 5%) had negligible influence on the ranking of top-performing wavelets, but resulted either in unnecessary narrowing or broadening of the candidate set. Therefore, the use of the 2% threshold is not arbitrary but reflects a practical and validated trade-off suitable for the current application. The DEV evolution for all mother wavelets is shown in Figure 6a. In Figure 6b, the DEV variation (%) values are shown.

$$DEV(\%) = \frac{DEVmax - DEV(n)}{DEVmax} \cdot 100 \quad (7)$$

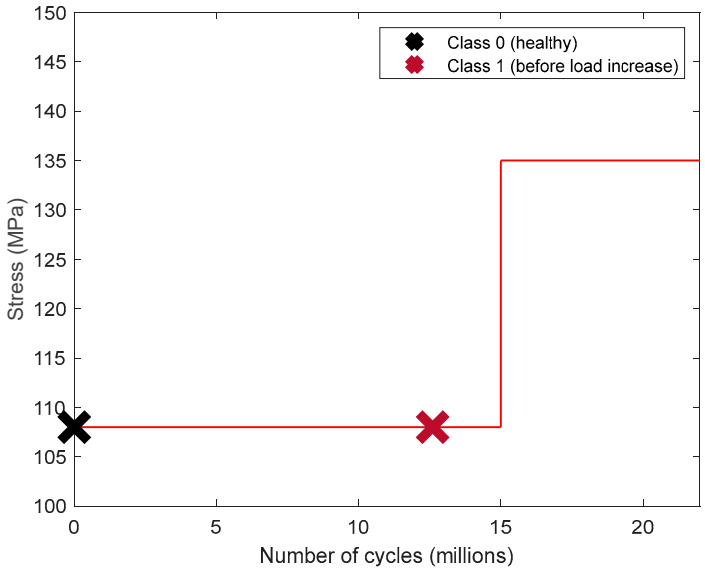

Figure 4. Considered classes for mother wavelet selection.

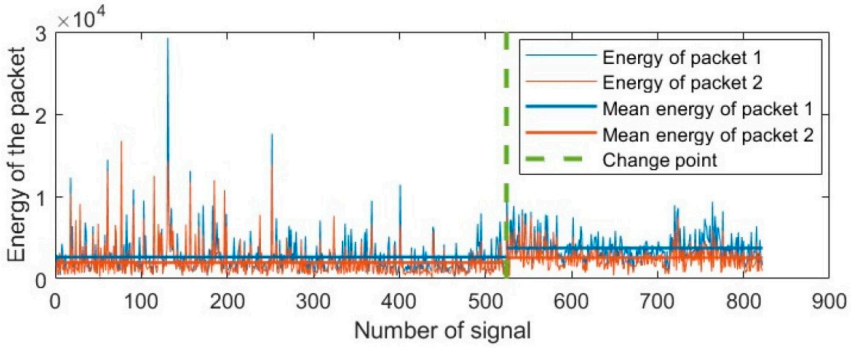

Figure 5. Mean energy of the packets for each selected signal and change point.

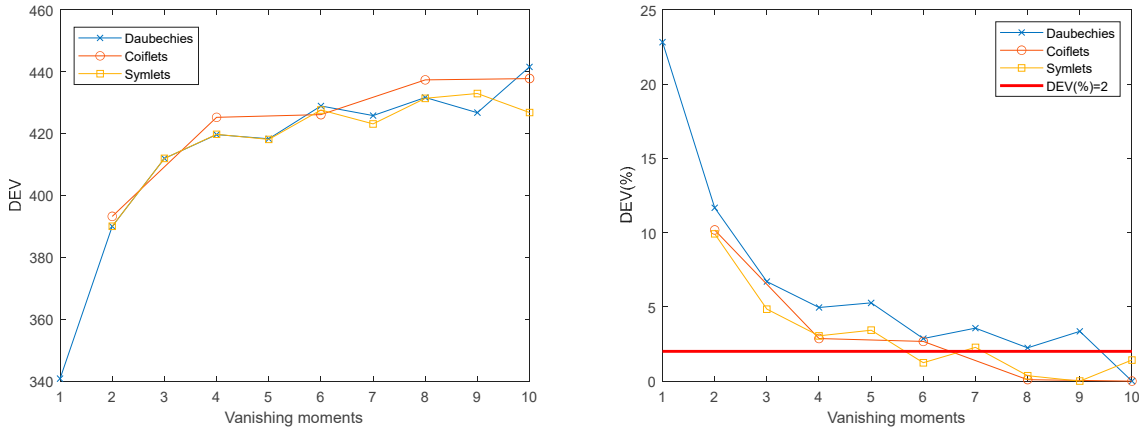

(**a**) (**b**)

Figure 6. DEV evolution of different families of mother wavelets: (**a**) Daubechies, Coiflets and Symlets; (**b**) DEV (%).

According to the previous criterion, for Daubechies family, the highest DEV is obtained with Daubechies 10 (Figure 6a) and below that order there is none of said family with a variation of less than 2% (Figure 6b), so only the db10 is preselected. For Symlets family, the highest DEV is obtained with sym9 (Figure 6a), and sym6, sym8 and sym10 have a DEV value with less than 2% variation (Figure 6b), so these mother wavelets are preselected for this family. About the Coiflets family, coiflet 5 (10 vanishing moments) and 4 (8 vanishing moments) are preselected for the same reasoning.

The packet energies obtained using the preselected mother wavelets are used as input for an intelligent classification system built with MATLAB R2024a®'s "Classification Learner" app [54]. This tool allows training and comparing multiple classification models under the same conditions. In this study, all the available models within the app were trained using the same dataset, and their performance was compared based on accuracy.

The model that achieved the highest success rate (i.e., classification accuracy) was the Ensemble Bagged Trees, which was, therefore, selected for further analysis. This model is also used to generate the comparison results presented in Table 2.

Ensemble methods like Bagged Trees improve predictive performance by combining multiple weak learners (in this case, decision trees) into a strong overall model [55,56]. Decision trees are intuitive, tree-structured models used to assign class labels based on input features. However, a single decision tree may be prone to overfitting or high variance. The concept of "bagging" (bootstrap aggregating) helps mitigate this by creating several random subsets of the training data (with replacement), training an individual tree on each subset, and then averaging the predictions of all trees. This aggregation process enhances robustness and overall accuracy compared to a single decision tree.

Table 2. Success rate of Ensemble Bagged Trees model for the preselected mother wavelets.

Mother Wavelet	Success Rate (%)
Db10	96.8
Coif4	95.6
Coif5	96.4
Sym6	95.6
Sym8	95.7
Sym9	96.0
Sym10	95.7

The choice to select the model with the highest accuracy is justified by the fact that accuracy is a widely accepted performance metric for classification tasks, especially when the dataset is balanced and the goal is to maximize correct classification across all classes. In this context, accuracy provides a reliable indication of the model's generalization capability.

The mother wavelet with the highest success rate will be the optimal for the study case.

Then, according to the highest success rates, db10 has been chosen as the optimal mother wavelet for this application, and it will be used in a further analysis to detect damage. In Figure 7a, the mother wavelet db10 is shown, and in Figure 7b, an example of a typical AE burst signal is represented. It can be seen that both functions are very similar. In Figure 7a, the time-domain representation of the db10 mother wavelet is shown, while Figure 7b displays a typical acoustic emission (AE) burst signal acquired during the test. Although the two functions are not identical, they share key morphological features that justify the suitability of db10 for this application. Both exhibit short-duration, asymmetric waveforms with rapid rise times, followed by decaying oscillations, a typical signature of transient, burst-type signals.

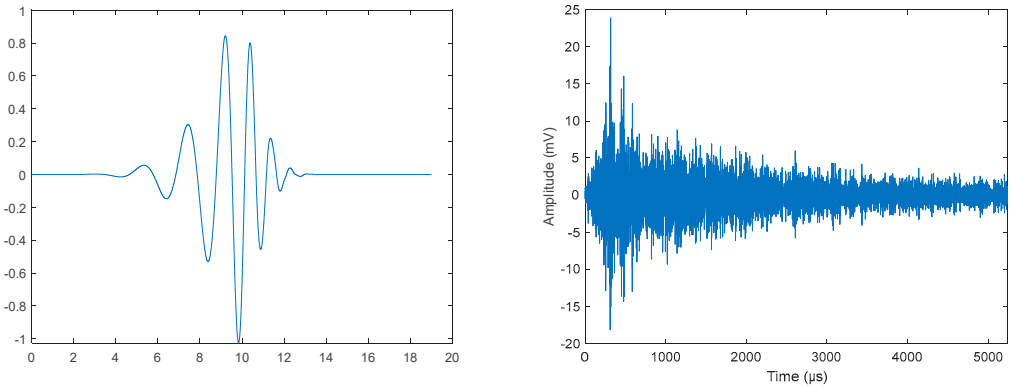

(**a**) (**b**)

Figure 7. Similarity of mother wavelet function to AE events: (**a**) Mother wavelet db10; (**b**) Example of AE burst signal.

The db10 wavelet, with its 10 vanishing moments and compact support, offers high time-frequency localization and is capable of representing signals with sharp transients and abrupt changes. This structural similarity facilitates the projection of AE signals onto the wavelet basis, enhancing the concentration of energy in a small number of coefficients during the WPT. Consequently, db10 allows efficient feature extraction and signal representation, particularly for damage-related AE events that manifest as short, high-energy bursts.

The confusion matrix of the model is shown in Figure 8. It reveals a high classification performance for both classes. Specifically, for class 0, the true positive rate (TPR) is 97.5%, meaning that the model correctly identifies 97.5% of the signals belonging to this class, while the false negative rate (FNR) is only 2.5%. Similarly, for class 1, the TPR is 95.6%, and the

FNR is 4.4%. These results indicate that the model is capable of accurately distinguishing between the two classes with minimal misclassification.

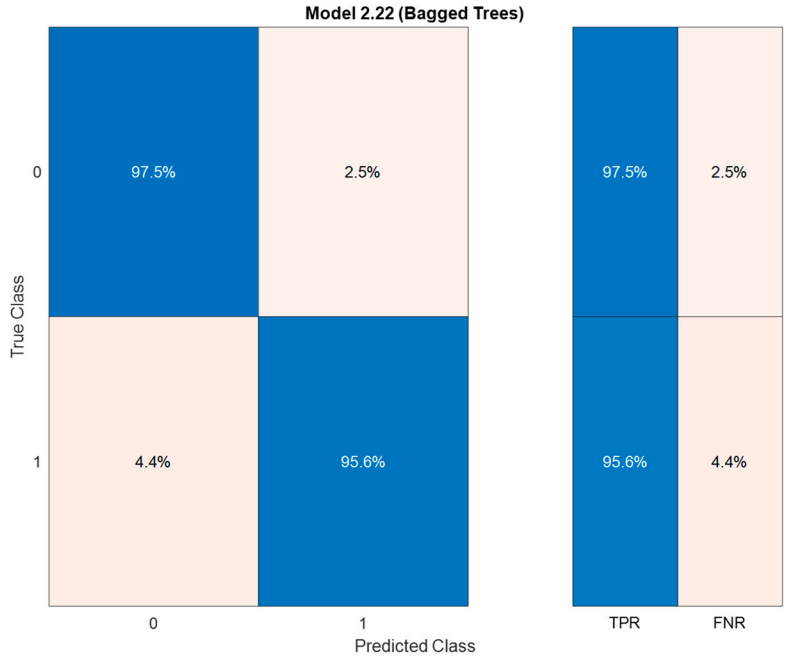

Figure 8. Confusion matrix of the Ensemble Bagged Trees (case of the db10 mother wavelet).

Given these high TPR values and low FNR values for both classes, the model demonstrates both sensitivity and reliability, which are essential for applications where distinguishing between signal types is critical. Furthermore, considering the use of the selected mother wavelet (db10), which is known for its ability to capture subtle signal features, the model's performance suggests an optimal feature extraction process. Therefore, it can be concluded that the model is not only valid, but also well-optimized for the studied case, providing a robust tool for signal classification within this context.

5. Post Processing of Acoustic Emission Raw Data

The WPT is applied using the selected mother wavelet db10 and a decomposition level of 3, resulting in 8 packets, which correspond to equally spaced sub-bands of the analyzed frequency range. This level of decomposition has proven to be sufficient to obtain clear and meaningful results, as supported by previous studies [25,27] and as it was previously explained.

Moreover, acoustic emission signals typically concentrate most of their energy in the lower frequency bands. Figure 9 shows the frequency analysis of the damage signal shown in Figure 7b. In is because the phenomena associated with damage initiation and progression (such as micro-crack formation or frictional events) generate transient, low-frequency components that are characteristic of the early stages of material degradation. As a result, a decomposition level of 3 captures the most informative part of the signal without introducing unnecessary computational complexity.

This choice not only ensures fast and reliable monitoring but also aligns with the configuration used during the mother wavelet selection stage, thus eliminating the need for additional parameter tuning or repeated calculations. This significantly reduces processing time, which is especially advantageous for real-time condition monitoring and early damage detection applications.

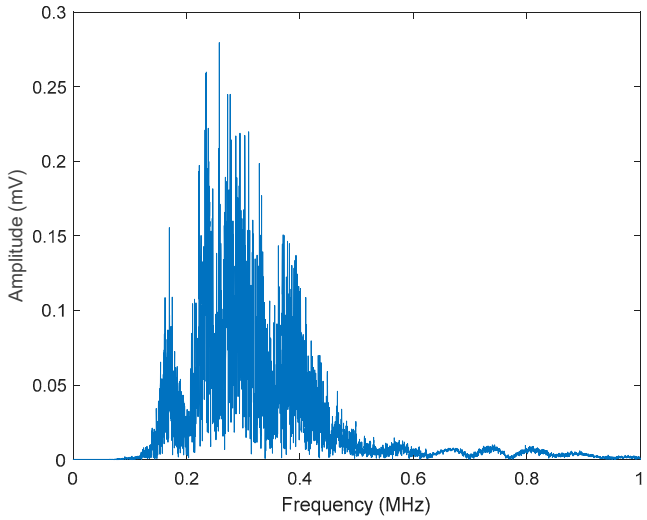

Figure 9. Frequency analysis of the damage signal shown in Figure 7b.

The Daubechies db10 mother wavelet was found to provide the best performance in this scenario. This can be theoretically justified by considering the specific characteristics of both the wavelet and the AE signals generated by fretting fatigue. Daubechies wavelets, including db10, are well-known for their high number of vanishing moments (10 in the case of db10), which confer excellent ability to represent signals with sharp transients and discontinuities. Such properties make db10 particularly suitable for capturing the burst-type AE waveforms that are typical of crack initiation events, characterized by abrupt changes in amplitude and frequency content. Moreover, the compact support of db10 allows efficient localization of signal features in both time and frequency domains, facilitating the extraction of meaningful energy distributions relevant to damage detection.

In Figure 10, the cumulative energy as a function of the number of cycles is shown for the complete set of AE signals (i.e., without dividing them into packets as performed previously). In this case, the WPT is applied to each signal as a whole. A significant increase in energy is observed just before 12 million cycles, marked by a red line in Figure 10. It is known from the literature that both failure initiation and final failure are characterized by a high energy level [57]. As it is known that the fracture takes place at the end of the test, the sudden energy increase may mean crack initiation. From a physical standpoint, the abrupt energy increase reflects the rapid release of elastic energy stored in the material as micro-cracks coalesce into a detectable fracture. This stage of crack progression is marked by higher-amplitude and more frequent AE events, which result in a sudden rise in signal energy. Therefore, the increase in energy not only signals the initiation of damage, but also correlates with the intensity of the underlying fracture mechanisms.

This observation is consistent with previous works, but with the added benefit that the current method works directly on raw AE data, making it a simpler and faster approach for in-service crack detection.

Furthermore, this methodology enables a straightforward procedure for future crack detection tasks: it is only necessary to apply the wavelet-based energy extraction method and monitor for significant changes in cumulative energy over time. The detection does not require signal segmentation, clustering, or manual interpretation, which enhances its applicability in real-time monitoring systems.

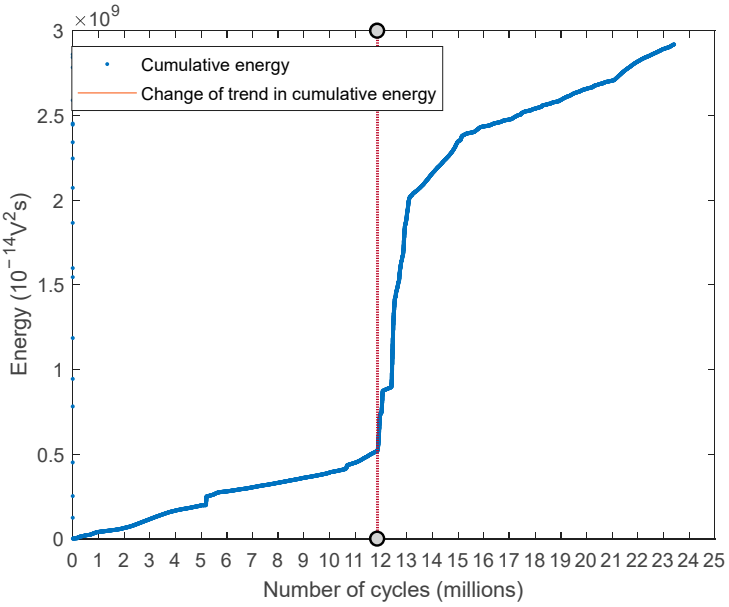

Figure 10. Cumulative WPT energy of the AE signals.

6. Conclusions

In this work, a procedure to detect crack initiation in a railway axle due to fretting fatigue has been developed. The proposed methodology is based on applying the Wavelet Packet Transform (WPT) to acoustic emission (AE) signals in order to analyze their energy distribution. To ensure the most efficient signal analysis, a selection procedure was conducted to identify the optimal mother wavelet for this application, resulting in the choice of the db10 wavelet, which demonstrated the highest classification performance and best class separation when used with a bagged trees model. This combination yielded not only a high success rate but also a low false alarm rate, making the classification both accurate and reliable.

Importantly, the energy of the packets was calculated at a decomposition level of 3, which strikes a balance between computational efficiency and feature resolution. This allowed for fast results, while the cumulative energy curve revealed a clear energy increase around 12 million cycles, potentially indicating crack initiation.

A key advantage of the proposed method lies in its ability to operate directly on raw AE data, avoiding the need for prior clustering or extensive post-processing. The wavelet transform effectively acts as a filter that highlights damage-related signal components, due to its adaptability to transient features typical of crack formation. As a result, the methodology enables automatic and real-time condition monitoring of the axle.

Moreover, the speed of the method is mainly due to its automated nature, which allows results to be obtained almost immediately. The methodology has been specifically optimized to provide the most reliable results in the shortest possible computation time, making it highly efficient for practical applications.

Author Contributions: Conceptualization, M.Z.; methodology, M.Z.; software, M.Z. and M.C.; validation, M.Z., M.J.G. and C.C.; formal analysis, M.Z.; investigation, M.Z. and M.C.; resources, M.C.; data curation, M.Z.; writing—original draft preparation, M.Z. and M.C.; writing—review and editing, M.Z. and M.C.; visualization, M.Z. and M.C.; supervision, M.C., M.J.G. and C.C.; project administration, M.C.; funding acquisition, M.Z. and M.C. All authors have read and agreed to the published version of the manuscript.

Funding: This research received no external funding.

Institutional Review Board Statement: Not applicable.

Informed Consent Statement: Not applicable.

Data Availability Statement: The original contributions presented in this study are included in the article. Further inquiries can be directed to the corresponding author.

Acknowledgments: The authors would like to thank S. Beretta and S. Cantini for the given support and the useful discussion and S. Bertozzi for the active help given to the research. PoliNDT (Inter-departmental Lab for Non-Destructive Testing and Structural Health Monitoring set at Politecnico di Milano) is also acknowledged for providing the acoustic emission equipment. M. Zamorano thanks Universidad Carlos III de Madrid for funding the visiting period at Politecnico di Milano to collaborate on the research work through the "Ayudas para la movilidad de investigadores de la UC3M en centros de investigación nacionales y extranjeros en sus dos modalidades 2022" project.

Conflicts of Interest: The authors declare no conflicts of interest. The funders had no role in the design of the study; in the collection, analyses, or interpretation of data; in the writing of the manuscript; or in the decision to publish the results.

Abbreviations

The following abbreviations are used in this manuscript:

AE	Acoustic Emission
COIF	Coiflet mother wavelet
CPA	Change Point Analysis
DB	Daubechies mother wavelet
DEV	Degree of Energy Variation
DWT	Discrete Wavelet Transform
EDM	Electrical Discharge Machining
FNR	False Negative Rate
NDT	non-destructive testing
PLB	Pencil Lead Break
SHM	Structural Health Monitoring
SYM	Symlet mother wavelet
TPR	True Positive Rate
UT	Ultrasonic Testing
WPT	Wavelet Packet Transform
WT	Wavelet Transform

References

1. *EN 13260:2020*; Railway Applications—Wheelsets and Bogies—Wheelsets—Product Requirements. European Committee for Standardization: Belgium, Brussels, 2020. Available online: https://standards.iteh.ai/catalog/standards/cen/2918a430-161a-4376-8927-f4df6fa45507/en-13260-2020 (accessed on 14 March 2023).
2. Section G—Wheels and Axle Manual (2020). Available online: https://aarpublications.com/section-g-wheels-and-axle-manual-2016g.html (accessed on 14 March 2023).
3. Waterhouse, R.B. Fretting Corrosion. In Proceedings of the Institution of Mechanical Engineers, London, UK, 14 January 1955.
4. Waterhouse, R.B. Fretting Fatigue. *Int. Mater. Rev.* **1992**, *37*, 77–98. [CrossRef]
5. Szolwinski, M.P.; Farris, T.N. Mechanics of Fretting Fatigue Crack Formation. *Wear* **1996**, *198*, 93–107. [CrossRef]
6. Zou, L.; Zeng, D.; Tian, X.; Jiang, G.; Dong, Y.; Zhao, H.; Lu, L. Experimental and Numerical Study on the Multi-Site Fretting Fatigue Crack Initiation of Press-Fitted Axles. *Fatigue Fract. Eng. Mater. Struct.* **2024**, *47*, 473–490. [CrossRef]
7. Nesládek, M.; Španiel, M.; Jurenka, J.; Růžička, J.; Kuželka, J. Fretting Fatigue—Experimental and Numerical Approaches. *Int. J. Fatigue* **2012**, *44*, 61–73. [CrossRef]
8. Dong, Y.; Zeng, D.; Zhao, H.; Wu, P.; Song, Y.; Li, X.; Lu, L. Fretting Fatigue Strength Evaluation of Scaled Press-Fitted Railway Axle Containing a Circumferential Groove Defect. *Int. J. Fatigue* **2025**, *194*, 108824. [CrossRef]
9. Gao, J.-W.; Dai, X.; Zhu, S.-P.; Zhao, J.-W.; Correia, J.A.F.O.; Wang, Q. Failure Causes and Hardening Techniques of Railway Axles—A Review from the Perspective of Structural Integrity. *Eng. Fail. Anal.* **2022**, *141*, 106656. [CrossRef]
10. Kwon, S.-J.; Seo, J.-W.; Choe, J.; Hong, S.-K. Fretting Crack Detection of a Railway Axle with a Mounted Wheel Using an Induced Current Potential Drop and Electromagnetic-Field Distribution. *J. Mech. Sci. Technol.* **2023**, *37*, 6453–6460. [CrossRef]

11. Xu, T.; Lu, L.; Zeng, D.; Zou, L. Fretting Fatigue Crack Growth Simulation and Residual Life Assessment of Railway Press-Fitted Axle. *Eng. Fract. Mech.* **2023**, *286*, 109290. [CrossRef]
12. García-Prada, J.C.; Castejon, C.; Gómez, M.J.; Alvarez, J.; Moreno, A.; Kappes, W. Euraxles-WP5: Non Destructive Testing (NDT) and Verification on the Reliability of Axles in Service. In Proceedings of the 17th International Wheelset Congress, Kiev, Ukraine, 22–27 September 2013.
13. Carboni, M.; Crivelli, D. An Acoustic Emission Based Structural Health Monitoring Approach to Damage Development in Solid Railway Axles. *Int. J. Fatigue* **2020**, *139*, 105753. [CrossRef]
14. Deng, X.-J.; Xui, G.-J.; Liu, S.-Q. Research on Fatigue Crack Detection of Rail Vehicle Axle Based on Acoustic Emission. *Struct. Health Monit.* **2015**, *2015*. [CrossRef]
15. Jiang, C.; Pan, S.; Zhang, C.; Li, F. Experimental Research on Fault Location for the Axle of Railway Vehicles Based on Acoustic Emission Technique. *Int. J. Control Autom.* **2016**, *9*, 91–98. [CrossRef]
16. Zhou, Y.; Lin, L.; Wang, D.; He, M.; He, D. A New Method to Classify Railway Vehicle Axle Fatigue Crack AE Signal. *Appl. Acoust.* **2018**, *131*, 174–185. [CrossRef]
17. Marks, R.; Stancu, A.; Soua, S. Fatigue Crack Growth Monitoring Using Acoustic Emission: A Case Study on Railway Axles. In Proceedings of the Advances in Condition Monitoring and Structural Health Monitoring, Singapore, 2–5 December 2019; Gelman, L., Martin, N., Malcolm, A.A., Liew, C.K., Eds.; Springer: Singapore, 2021; pp. 551–560.
18. Rolek, P.; Bruni, S.; Carboni, M. Condition Monitoring of Railway Axles Based on Low Frequency Vibrations. *Int. J. Fatigue* **2016**, *86*, 88–97. [CrossRef]
19. Gómez, M.J.; Castejón, C.; Corral, E.; García-Prada, J.C. Railway Axle Condition Monitoring Technique Based on Wavelet Packet Transform Features and Support Vector Machines. *Sensors* **2020**, *20*, 3575. [CrossRef]
20. Chong, S.Y.; Shin, H. A Review of Health and Operation Monitoring Technologies for Trains. *SMART Struct. Syst.* **2010**, *6*, 1079–1105. [CrossRef]
21. Lanzagorta, J.L.; Aizpurua, I.; Vázquez, P.R.; Castro, I. New Ways to Inspect Railway Axles: From Simulation to Experimental Validation. *NDT E Int.* **2021**, *121*, 102439. [CrossRef]
22. Carboni, M.; Zamorano, M. On MONITORING fretting Fatigue Damage in Solid Railway Axles by Acoustic Emission with Unsupervised Machine Learning and Comparison to Non-Destructive Testing Techniques. *Proc. Inst. Mech. Eng. Part F J. Rail Rapid Transit.* **2024**, *238*, 256–267. [CrossRef]
23. Grosse, C.U.; Ohtsu, M.; Aggelis, D.G.; Shiotani, T. (Eds.) *Acoustic Emission Testing*; Springer: Berlin/Heidelberg, Germany, 2008; ISBN 978-3-540-69895-1.
24. Deshpande, A.; Kumar, M. *Artificial Intelligence for Big Data: Complete Guide to Automating Big Data Solutions Using Artificial Intelligence Techniques*; Packt Publishing Ltd.: Birmingham, UK, 2018; ISBN 978-1-78847-601-0.
25. Zamorano, M.; Gómez Garcia, M.J.; Castejón, C. Selection of a Mother Wavelet as Identification Pattern for the Detection of Cracks in Shafts. *J. Vib. Control* **2022**, *28*, 3152–3161. [CrossRef]
26. Wai Keng, N.; Leong, M.; Hee, L.; Abdelrhman, A. Wavelet Analysis: Mother Wavelet Selection Methods. *Appl. Mech. Mater.* **2013**, *393*, 953–958. [CrossRef]
27. Zamorano, M.; Avila, D.; Marichal, G.N.; Castejon, C. Data Preprocessing for Vibration Analysis: Application in Indirect Monitoring of 'Ship Centrifuge Lube Oil Separation Systems'. *J. Mar. Sci. Eng.* **2022**, *10*, 1199. [CrossRef]
28. Grosse, C.U.; Reinhardt, H.W.; Motz, M.; Kroplin, B. Signal Conditioning in Acoustic Emission Analysis Using Wavelets. *NDT. Net.* **2002**, *7*, 1–9. Available online: https://www.ndt.net/article/v07n09/08/08.htm (accessed on 14 March 2023).
29. Ebrahimian, Z.; Ahmadi, M.; Sadri, S.; Li, B.Q.; Moradian, O. Wavelet Analysis of Acoustic Emissions Associated with Cracking in Rocks. *Eng. Fract. Mech.* **2019**, *217*, 106516. [CrossRef]
30. Barbosh, M.; Dunphy, K.; Sadhu, A. Acoustic Emission-Based Damage Localization Using Wavelet-Assisted Deep Learning. *J. Infrastruct. Preserv. Resil.* **2022**, *3*, 6. [CrossRef]
31. Kek, T.; Kusić, D.; Grum, J. Wavelet Packet Decomposition to Characterize Injection Molding Tool Damage. *Appl. Sci.* **2016**, *6*, 45. [CrossRef]
32. Wang, C.H. *Introduction to Fracture Mechanics*; DSTO Aeronautical and Maritime Research Laboratory: Victoria, Australia, 1996.
33. Chai, M.; Hou, X.; Zhang, Z.; Duan, Q. Identification and Prediction of Fatigue Crack Growth under Different Stress Ratios Using Acoustic Emission Data. *Int. J. Fatigue* **2022**, *160*, 106860. [CrossRef]
34. Beale, C.; Niezrecki, C.; Inalpolat, M. An Adaptive Wavelet Packet Denoising Algorithm for Enhanced Active Acoustic Damage Detection from Wind Turbine Blades. *Mech. Syst. Signal Process.* **2020**, *142*, 106754. [CrossRef]
35. Liu, T.; Jin, Y.; Wang, S.; Zheng, Q.; Yang, G. Denoising Method of Weak Fault Acoustic Emission Signal under Strong Background Noise of Engine Based on Autoencoder and Wavelet Packet Decomposition. *Struct. Health Monit.* **2023**, *22*, 3206–3224. [CrossRef]
36. Zhao, Y.; Ma, Y.; Du, J.; Wang, C.; Xia, D.; Xin, W.; Zhan, Z.; Zhang, R.; Chen, J. Noise Reduction Based on a CEEMD-WPT Crack Acoustic Emission Dataset. *Appl. Sci.* **2023**, *13*, 10274. [CrossRef]

37. Wang, Z.; Ding, K.; Ren, H.; Ning, J. Quantitative Acoustic Emission Investigation on the Crack Evolution in Concrete Prisms by Frequency Analysis Based on Wavelet Packet Transform. *Struct. Health Monit.* **2022**, *21*, 1046–1060. [CrossRef]
38. Workman, G.L.; Kishoni, D.; Moore, P.O. (Eds.) *Ultrasonic Testing*; American Society for Nondestructive Testing: Columbus, OH, USA, 2007; ISBN 978-1-57117-163-4.
39. Gao, L.; Wang, H.; Zhou, J.; Zhou, X. Selection of Optimal Mother Wavelet for Acoustic Emission Signal Processing of Gas Pipeline Leakage. In Proceedings of the TEPEN 2022, Baotou, China, 18–21 August 2022; Zhang, H., Ji, Y., Liu, T., Sun, X., Ball, A.D., Eds.; Springer Nature: Cham, Switzerland, 2023; pp. 294–305.
40. Foletti, S.; Beretta, S.; Gurer, G. Defect Acceptability under Full-Scale Fretting Fatigue Tests for Railway Axles. *Int. J. Fatigue* **2016**, *86*, 34–43. [CrossRef]
41. Foletti, S.; Beretta, S.; Bertozzi, F.; Carboni, M.; Cervello, S.; Regazzi, D. Experiments on Crack Propagation and Threshold at Defects in Press-Fits of Railway Axles. *Procedia Struct. Integr.* **2017**, *7*, 484–491. [CrossRef]
42. Pourheidar, A.; Regazzi, D.; Cervello, S.; Foletti, S.; Beretta, S. Fretting Fatigue Analysis of Full-Scale Railway Axles in Presence of Artificial Micro-Notches. *Tribol. Int.* **2020**, *150*, 106383. [CrossRef]
43. *EN 13261:2020*; Railway Applications—Wheelsets and Bogies—Axles—Product Requirements. British Standards Institution: London, UK, 2020. Available online: https://standards.iteh.ai/catalog/standards/cen/30ad3acd-39c1-4372-a5a4-69892c4d555d/en-13261-2020 (accessed on 14 March 2023).
44. Hirakawa, K.; Toyama, K.; Kubota, M. The Analysis and Prevention of Failure in Railway Axles. *Int. J. Fatigue* **1998**, *20*, 135–144. [CrossRef]
45. Cervello, S. Fatigue Properties of Railway Axles: New Results of Full-Scale Specimens from Euraxles Project. *Int. J. Fatigue* **2016**, *86*, 2–12. [CrossRef]
46. *E976-15(2021)*; Committee Guide for Determining the Reproducibility of Acoustic Emission Sensor Response. ASTM International: West Conshohocken, PA, USA, 2021.
47. Mallat, S. *A Wavelet Tour of Signal Processing*; Academic Press: Cambridge, MA, USA, 1999; ISBN 978-0-12-466606-1.
48. Riabova, S. Application of Wavelet Analysis to the Analysis of Geomagnetic Field Variations. *J. Phys. Conf. Ser.* **2018**, *1141*, 012146. [CrossRef]
49. Jensen, A.; la Cour-Harbo, A. *Ripples in Mathematics*; Springer: Berlin/Heidelberg, Germany, 2001; ISBN 978-3-540-41662-3.
50. Zamorano, M.; Gómez, M.J.; Castejón, C. Optimal Selection of the Mother Wavelet in WPT Analysis and Its Influence in Cracked Railway Axles Detection. *Machines* **2023**, *11*, 493. [CrossRef]
51. Castejón, C.; Lara, O.; GARCIA-PRADA, J.C. Automated Diagnosis of Rolling Bearings Using MRA and Neural Networks. *Mech. Syst. Signal Process.* **2010**, *24*, 289–299. [CrossRef]
52. Hernández, A.; Castejón, C.; García-Prada, J.C.; Padrón, I.; Marichal, G.N. Wavelet Packets Transform Processing and Genetic Neuro-Fuzzy Classification to Detect Faulty Bearings. *Adv. Mech. Eng.* **2019**, *11*, 1687814019831185. [CrossRef]
53. Taylor, W. *Change-Point Analysis: A Powerful New Tool For Detecting Changes*; Report No. M38.1; Baxter Healthcare Corporation: Deerfield, IL, USA, 2000; Available online: https://variation.com/wp-content/uploads/change-point-analyzer/change-point-analysis-a-powerful-new-tool-for-detecting-changes.pdf (accessed on 28 July 2025).
54. MathWorks. *Machine Learning Toolbox*, Version 12.4; MathWorks: Natick, MA, USA, 2024. Available online: https://www.mathworks.com/products/statistics.html (accessed on 28 July 2025).
55. Ullah, Z.; Saleem, F.; Jamjoom, M.; Fakieh, B. Reliable Prediction Models Based on Enriched Data for Identifying the Mode of Childbirth by Using Machine Learning Methods: Development Study. *J. Med. Internet Res.* **2021**, *23*, e28856. [CrossRef]
56. Smith, T.C.; Frank, E. Introducing Machine Learning Concepts with WEKA. *Methods Mol. Biol. Clifton.* **2016**, *1418*, 353–378. [CrossRef]
57. Marfo, A.; Chen, Z.; Li, J. Acoustic Emission Analysis of Fatigue Crack Growth in Steel Structures. *J. Civ. Eng. Constr. Technol.* **2013**, *4*, 239–249. [CrossRef]